Eur. Phys. J. D (2013) 67: 128
DOI: 10.1140/epjd/e2013-30769-2

THE EUROPEAN PHYSICAL JOURNAL D

Regular Article

Study of the effect of pyrex and quartz insulators on X-ray intensity in a 4 kJ plasma focus device

Saeedeh Koohestani, Morteza Habibi[a], and Reza Amrollahi

Department of Energy Engineering & Physics, AmirKabir University of Technology, Iran

Received 26 December 2012 / Received in final form 18 March 2013
Published online 27 June 2013 – © EDP Sciences, Società Italiana di Fisica, Springer-Verlag 2013

Abstract. In this paper we study the soft X-ray (SXR) and hard X-ray (HXR) intensity produced in different insulator sleeves by a 4 kJ plasma focus device (APF) using filtered PIN-diodes and a fast scintillation detector. The experiments were performed for a great number of neon filling gas pressures at voltages of 11, 12 and 13 kV. Lengths of 40 and 50 mm look optimal to yield the most SXR intensity for the Pyrex and Quartz insulators respectively. The device appears to optimize much better for Pyrex insulator than the Quartz. For Pyrex and Quartz insulators, the lengths of 40 mm and 50 mm seem optimal to yield maximum HXR intensity, respectively.

1 Introduction

Following the discovery of X-ray by Röntgen in 1895, this radiation brought about three chief branches of science: radiography, X-ray crystallography and X-ray spectrometry. Soft X-ray (SXR) sources are also essential for X-ray lithography (neon SXR ∼1−1.5 keV), microscopy (250−2500 eV) and micromachining (argon X-rays ∼4 keV). The plasma focus device (PFD) is a pulsed plasma generating device which produces a pinched plasma column in radial compression via a self-generated magnetic field [1,2]. This device has been studied since the early 1960s, and its use in research has been inspired from the early days by the ease of its engineering and its properties as a pulsed, cheap, and intense source of X-rays, relativistic electrons, energetic ions and fast neutrons [1–3]. In the PFD configuration as presented in Figure 1, when the discharge is started the gas breaks down at the insulator sleeve surface and the plasma current sheath flows toward the end of the anode due to the Lorentz force ($J_r \times B_\theta$). The electrical breakdown along the insulator is crucial for the formation of a homogeneous and symmetric current sheath [4] that is important for good plasma pinching and X-ray emission. The X-ray emission from the device is divided into three elements. The first is SXRs, which are radiated from the pinched plasma with wavelength $\lambda > 6$ Å (energy <2 keV). The source of this component is chiefly the neon plasma. The second element refers to characteristic line radiation from the neon plasma that is Ne and He Ly-α lines of wavelengths around 3.73−3.94 Å (3.15−3.32 keV). The third element is harder X-rays, caused by electron bombardment of the copper anode. This is characterised by the Cu K-α line of 1.43 Å (8.67 keV) [5]. The X-ray emission from a PFD depends in a relatively complex way upon the design and operating factors such as the applied voltage and bank energy, the circuit inductance [6], the working gas nature and pressure [7], the anode geometry and its material [8], the material and configuration of insulator sleeve [9] and the preionization assisted breakdown. So we need to investigate the affect of these factors on X-ray emission more comprehensively. Several studies have been devoted to the investigation of the effects of anode and insulator materials on SXRs and neutrons emitted by the device. The effect of the PFD insulator length on HXR intensity is reported in our previous paper [10]. Hussain et al. investigated the influence of insulator material on X-ray emission [11]. The effect of the insulator length on different characteristic timings of discharges was studied by Zhang et al. [12]. Rawat et al. studied the effect of the insulator sleeve length on SXR emission [13]. Serban and Lee studied temporal characteristics of the SXR emission through filtered PIN-diodes. They also showed that X-ray yield is equal to $I_p^2 v_{axial}^2$ in which v_{axial} and I_p are the axial speed of the current sheath and the current peak respectively [14]. Shyam and Rout investigated the effect of insulating and special anode materials on pinch current and neutron yield in a 2.2 kJ plasma focus device [15]. They focused on electrode material evaporation phenomena during the plasma focus operation and the coating of metal vapor on the insulator surface. In their study they concluded that for low energy plasma focus quartz or glass turns out to be a better insulator than alumina. Influence of insulator contamination by evaporation on neutron yield with a 2.3 kJ plasma focus device was investigated by Zakaullah et al. [16]. They reported that deposition of evaporated copper on the insulator surface reduces the neutron yield. The precise mechanisms by

[a] e-mail: mortezahabibi@aut.ac.ir

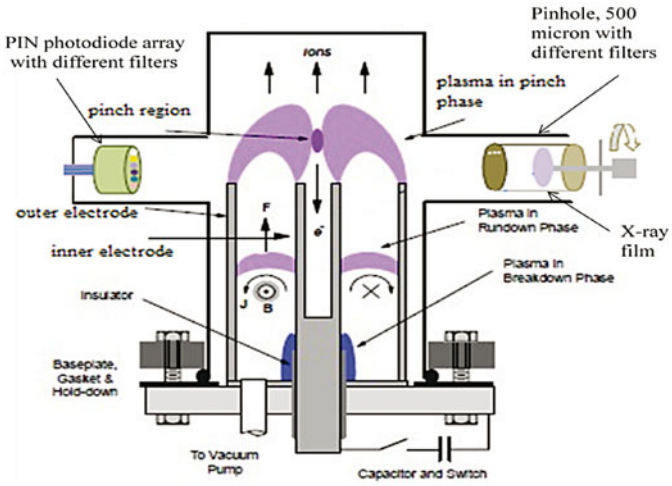

Fig. 1. Schematic view of the APF plasma focus with the pinhole camera and the PIN photo diode as diagnostics of soft X-rays.

which X-rays are emitted in the focused plasma column are still debated and more work is required to optimise the PFD as a cost-effective X-ray generator.

Modification of the insulator configuration of the PFD is almost always needed: even though theoretical analyses and numerical simulations provide helpful hints, optimised design of the insulator comes mainly from experimental trial and error. The main objective of the current work is to optimise the X-ray intensity (average area under the curve) from a neon filled single shot PFD by varying the length and the material of the insulator sleeve used at the closed end of the coaxial electrode assembly.

2 Experimental setup and diagnostics

Experiments were carried out on the APF Mather-type plasma focus device sited at the Amirkabir University of Technology [17]. The APF device is energised by a 40 μF capacitor charged up to 15 kV. The total measured external inductance is 115 nH. The copper anode is 148 mm long and 20 mm thick. The cathode is in the form of a squirrel cage containing 6 copper rods arranged concentrically around the anode with an inner diameter of 44.7 mm and a length of 145 mm. Pyrex insulators with effective lengths of 3, 3.5, 4, 4.5, 5, 5.5, and 6 cm and Quartz insulators with effective lengths of 3.5, 4, 4.5 and 5 cm were used in this study. The vacuum system consists of a rotary backed diffusion pump which evacuates the compartment down to 10^{-5} Torr before neon gas is introduced. After about five shots, the old gas is purged and fresh gas is added to reduce the effects of impurities gathered in the working gas as much as possible. Identical RG 58 Al shielded cables of length 8 m were used for all electrical diagnostics. In order to reduce the effects of electromagnetic (EM) noise on data signals, all cables were wrapped with Al foil. Four 100 and 200 MHz Tektronix oscilloscopes were used to record the signals from the diagnostic cables. The total discharge current was measured

Table 1. An array of four PIN photodiodes masked with filters.

PIN Diode	Filter	Thickness (μm)
1	Al + Mylar	12
2	Al + Mylar	24
3	Be	150
4	Cu	10

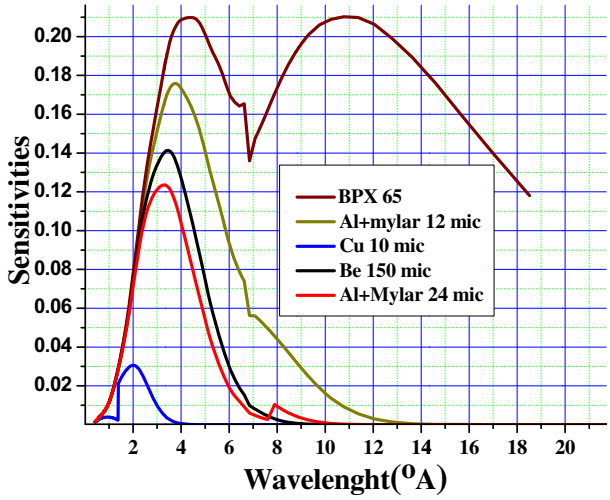

Fig. 2. The energy response of the PIN-diodes using different filters.

with a Rogowski coil. An array of four filtered PIN photodiodes (BPX-65) housed at 22 cm from the anode head were used to measure the SXR emissions from the focused plasma. For X-ray detection the glass windows of the PIN diodes were detached. The filters used for masking the PIN-diodes are shown in Table 1. The thickness of the Aluminium layers in 6 μm, 12 μm and 24 μm Al-Mylar foils are 2 μm, 5 μm, and 9 μm respectively. Each diode was reverse biased by 40 V. The energy response of the BPX-65 PIN photodiodes with and without their related absorption filters are shown in Figure 2. The PIN diodes which are masked with Al-Mylar 12 and 24 μm filters have a maximum of 3.3 keV and 3.6 keV, respectively. The maximum sensitivity of a detector filtered with Be 150 μm is at 3.6 keV and the detector filtered with Cu 10 μm transmits maximum X-rays with the energy of 6.3 keV. Furthermore the detectors were normalised against each other by masking each with an identical 10 μm aluminum filter. For the time resolved hard X-ray measurement a scintillator-photomultiplier detector composed of a NE-102 cylindrical (50 mm $\times$ 50 mm) plastic scintillator with 5 ns time resolution coupled with a photomultiplier (PM-53) biased at -1.3 kV is used. This detector is located outside of the discharge chamber, in front of a 5 mm glass window. In these experiments, discharges have been photographed by means of an X-ray pin-hole camera with a 500 μm diameter pin-hole aperture covered by Al-Mylar 6, 12 and 24 μm filters. The pin-hole camera is located in a radial position, viewing the plasma region and the top of the anode as well. The distance from the source to the pin-hole aperture is 21 cm and the distance from the

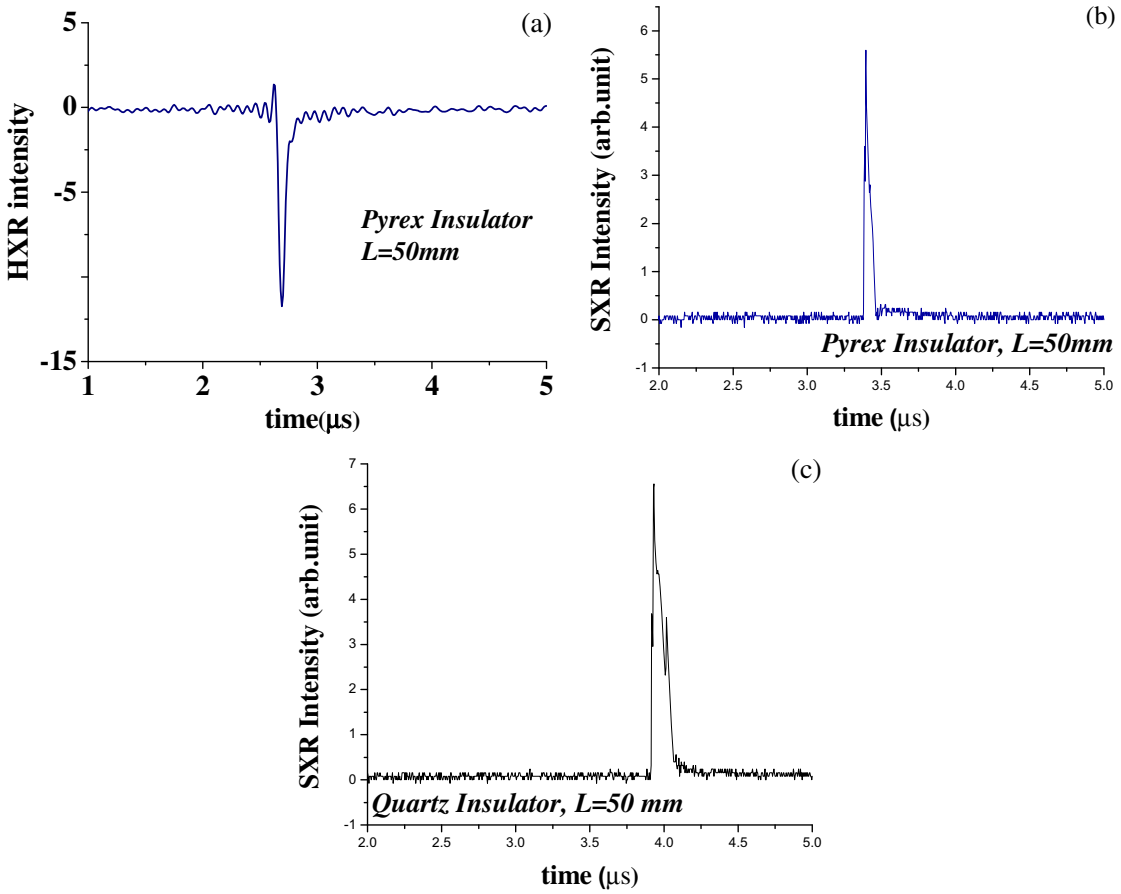

Fig. 3. Typical signals of (a) HXRs, (b) SXR with Pyrex insulator, (c) SXRs with a Quartz insulator.

aperture to the recording film is 5.2 cm, then the magnification factor of the image of the soft X-ray source is 0.248. The analysis as carried out using ORIGIN software and the MATLAB based signal acquisition program (SAP) designed by AmirKabir Fusion Lab.

3 Experimental results and discussion

In these experiments neon is used as the filling gas. Some conditioning shots are fired at the optimum pressure value before recording the data, to ensure that the readings are recorded under the best conditions. The data has been recorded at 11, 12, and 13 kV and at pressures of 6, 7 and 8 Torr. Also the data were averaged for five discharges. In Figure 3, typical SXR signals detected by Al + mylar 12 μm filtered PIN-diode and the HXR signal are depicted according to different insulator sleeves. To examine the influence of the insulator material on X-ray emission, the PFD was operated using Pyrex glass, Quartz, Plexi, Polyamide, and Teflon insulators. Incidentally neither focus nor X-ray emission was observed for Polyamide, Plexi and Teflon insulator sleeves. This may be due to improper breakdown discharge across the insulator. An observation was made of good focus and X-ray emission for Pyrex glass and Quartz insulators. The filling pressure

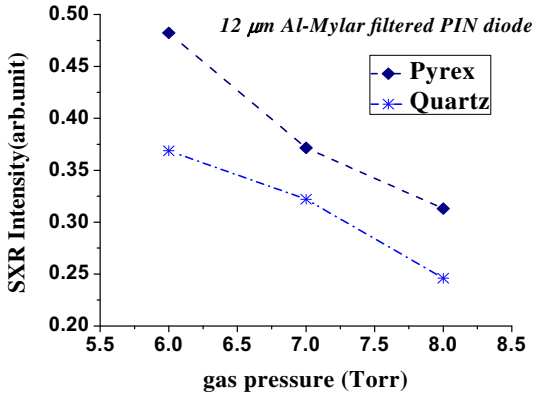

Fig. 4. The variation of X-ray intensity with gas pressure for Pyrex and Quartz insulator sleeve materials.

for all insulator sleeves ranges from 6 to 8 Torr, irrespective of the material. The variation of the X-ray intensity as a function of filling pressure measured by the PIN-diode filtered with Al-Mylar 12 μm is plotted in Figure 4. Each data point is created by averaging five successful discharges. The graph shows that for these insulator materials, X-ray emission rises with pressure up to a particular value and then declines. Also the X-ray emission is larger for the Pyrex insulator than for the Quartz insulator over

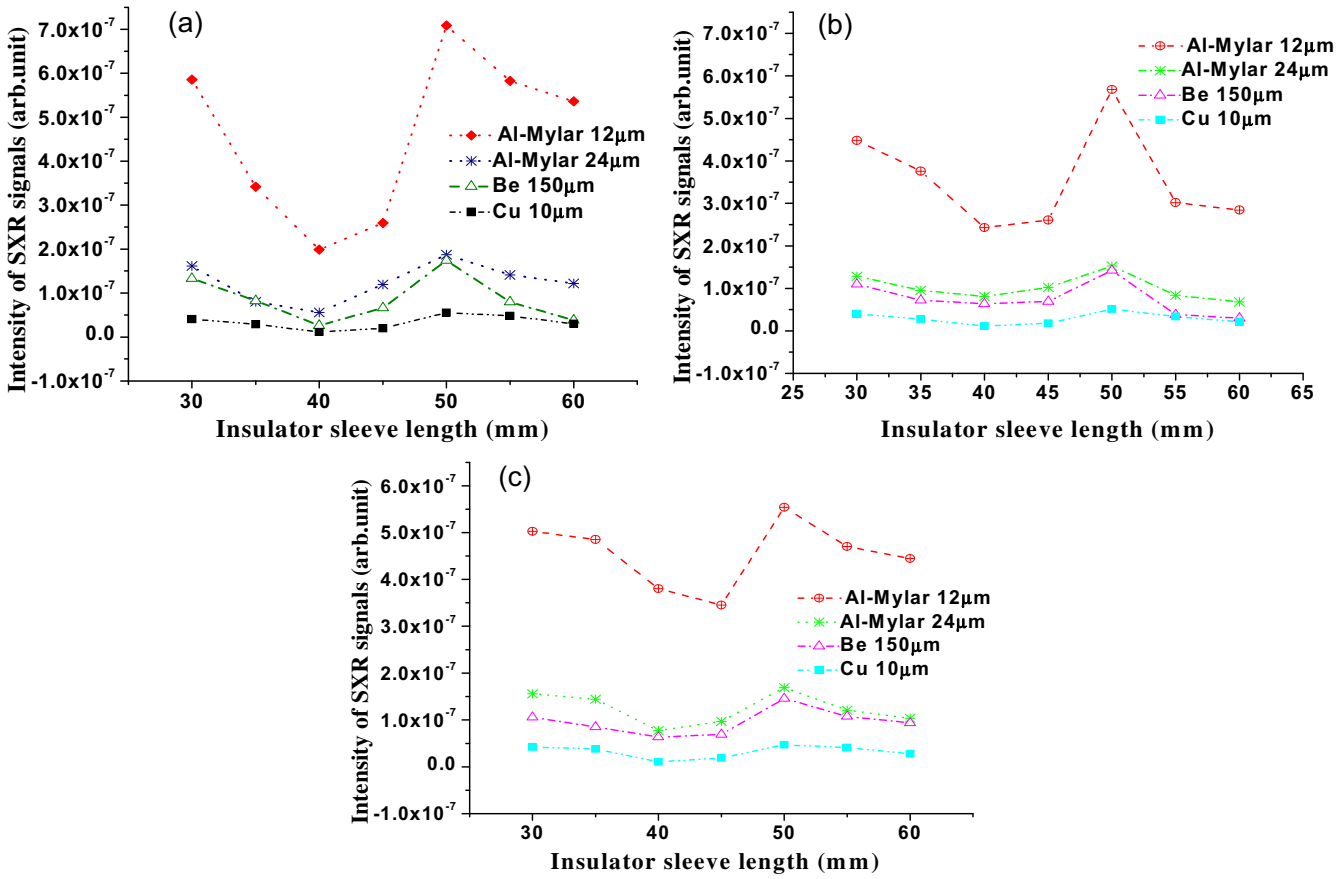

Fig. 5. Variation of SXR intensity with insulator length for Pyrex insulators under different working conditions: $V = 11$ kV, (a) $P = 6$ Torr, (b) $P = 7$ Torr, (c) $P = 8$ Torr.

the whole pressure range. In Figures 5 and 6, the SXR intensity obtained by different filtered PIN-diodes is plotted for various lengths of the Pyrex and Quartz insulators. Obviously the change in insulator length can influence the SXR intensity. The average SXR intensity has been found to increase with an increase of the Pyrex insulator length from 40 to 50 mm. A further increase in insulator length to 60 mm results in a decrease of the SXR intensity. The Quartz insulators have a different performance compared to the Pyrex insulators and SXR intensity is least for the 50 mm length. When the 40 mm Quartz insulator was used instead of the 35 mm, SXR intensity was enhanced and, by increasing the length of the insulator to 45 and 50 mm, the signal intensity was found to decrease. Thus, for the maximum production of SXRs lengths of 40 and 50 mm would seem best for the Pyrex Quartz insulators respectively. From Figures 5 and 6 it can be concluded that the Pyrex insulators would cause more SXR intensity than the Quartz insulators. Zakaullah et al. [18] have also studied the effect of insulator length on neutron yield. For neutrons, they demonstrated that there is an optimum insulator length where the neutron yield is the highest, just as we have observed for neon SXRs. As illustrated in Figure 7, to obtain the highest intensity of HXRs for Pyrex and Quartz insulators, the optimal length of the insulator would be equal to 50 mm and 40 mm respectively [10]. These results are in good agreement with the results of SXR intensity. One can conclude that the general behaviors seen in the plots of Figures 5 and 6 are the same and the only difference is in the amount of detected X-rays in which the 12 μm Al-Mylar and Cu 10 μm have the maximum and minimum amount, respectively.

In these experiments we have photographed discharges using an X-ray pinhole camera with 500 μm diameter pinhole apertures covered by Al-Mylar filters 6 and 12 μm thick. Figure 8 shows the X-ray images of the pinch region for the Quartz and Pyrex insulators with different lengths. The results from the pin-hole camera are in agreement with the SXR signals registered by the PIN diodes. It can be concluded that the quality of plasma column formation is related to SXR intensity. It had been shown that for all the charging voltages for various insulator lengths; there is an optimum pressure which produces a maximum X-ray intensity. As it is known, soft X-ray and neutron yield strongly depend on the curvature of the current sheath and the curvature of the current sheath has a correlation with the dimension of the device, especially with the insulator. When the sleeve is too long, the increase in inductance may cause the current sheath to remain at the insulator surface for a longer period of time, and alternatively when it is too short, the rapid current sheath development may cause spoke formation [19]. Therefore

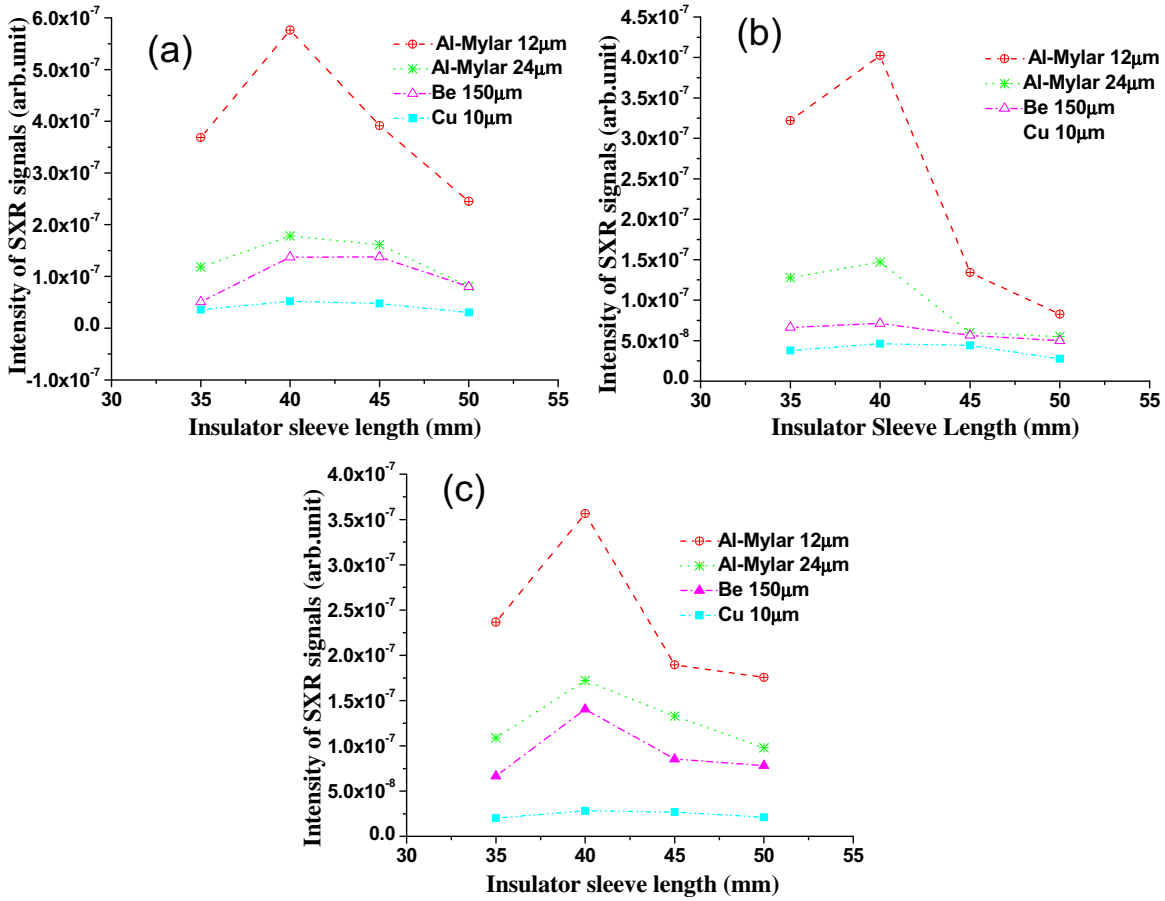

Fig. 6. Variation of SXR intensity with insulator length for Quartz insulators under different working conditions: $V = 11$ kV, (a) $P = 6$ Torr, (b) $P = 7$ Torr, (c) $P = 8$ Torr.

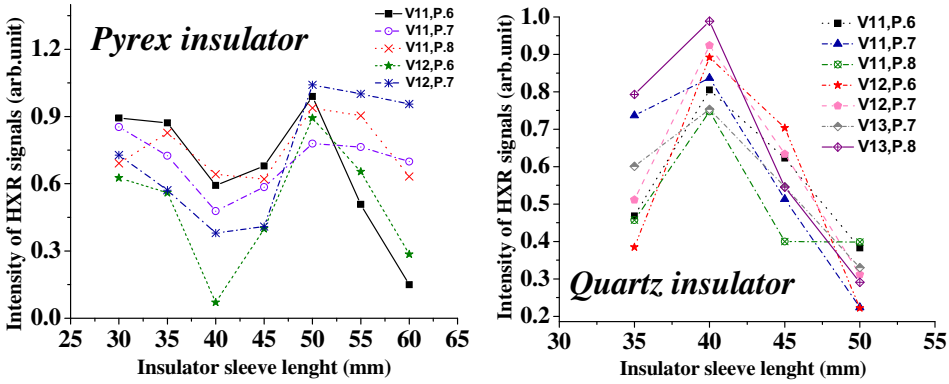

Fig. 7. Variation of HXR intensity with insulator length for Quartz and Pyrex insulators under different working conditions.

the insulator sleeve that surrounds part of the inner electrode has an important role in the plasma focus dynamics.

4 Conclusion

Our study revealed a strong correlation between the filling gas pressure, the insulator sleeve length, and the X-ray intensity. The SXR intensity was relatively low whenever the insulator length deviated from the optimum value. For the Quartz insulator the average SXR intensity has been proven to increase with an increase in insulator length from 35 mm to 40 mm but a further increase in insulator length to 50 mm resulted in a decrease in the SXR intensity. Regard the Pyrex insulator, the SXR intensity decreased as the length of the insulator increased from 30 mm to 40 mm but as it increased from 40 mm to 50 mm the SXR intensity increased. Lengths of 40 mm and 50 mm seem optimal to yield maximum HXR intensity for the Pyrex and Quartz insulators, respectively which confirms

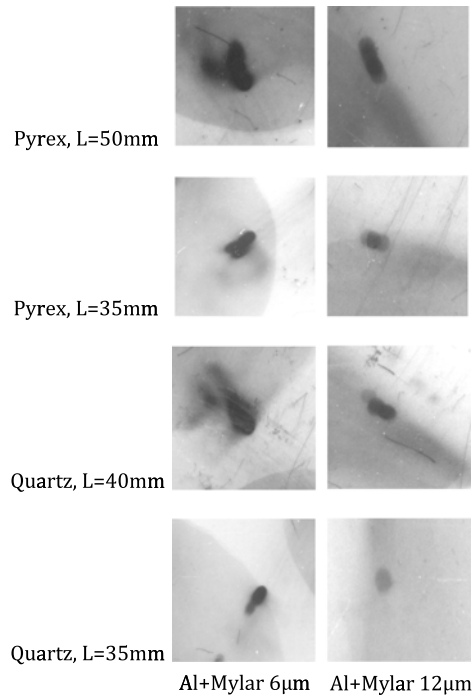

Fig. 8. X-Ray photographs of the plasma column taken by the pin-hole camera with two 500 μm apertures masked by 6 and 12 μm Al-Mylar filters at $V = 11$ kV, $P = 8$ Torr.

the results of SXR intensity. It should be emphasised that the insulator length has an important role in the effective performance of PFDs.

References

1. J.W. Mather, Phys. Fluid. **11**, 3 (1968)
2. J.M. Mather, Methods Exp. Phys. B **9**, 187 (1971)
3. S. Lee, T.Y. Tou, S.P. Moo, M.A. Eissa, A.V. Gholap, K.H. Kwek, S. Mulyodrono, A.J. Smith, S. Suryadi, W. Usada, M. Zakaullah, Am. J. Phys. **56**, 62 (1988)
4. G. Rosenman, D. Shur, J. Appl. Phys. **88**, 6109 (2000)
5. G.R. Etaati, R. Amrollahi, M. Habibi, K.H. Mohammadi, R. Baghdadi, A. Roomi, J. Fusion Energ. **29**, 503 (2010)
6. M. Liu, X. Feng, S.V. Springham, S. Lee, IEEE Trans. Plasma Sci. **26**, 135 (1998)
7. M. Zakaullah, K. Alamgir, G. Murtaza, A. Waheed, Plasma Sources Sci. Technol. **9**, 592 (2000)
8. S. Hussain, M. Shafiq, R. Ahmad, A. Waheed, M. Zakaullah, Plasma Sources Sci. Technol. **14**, 61 (2005)
9. R.S. Rawat, T. Zhang, C.B.L. Phua, J.X.Y. Then, K.A. Chandra, X. Lin, A. Patran, P. Lee, Plasma Sources Sci. Technol. **13**, 569 (2004)
10. S. Koohestani, M. Habibi, R. Amrollahi, R. Baghdadi, A. Roomi, J. Fusion Energ. **30**, 68 (2011)
11. S. Hussain, M. Shafiq, M.A. Badar, M. Zakaullah, Phys. Plasmas **17**, 092705 (2010)
12. T. Zhang, X. Lin, K.A. Chandra, T.L. Tan, S.V. Springham, A. Patran, P. Lee, S. Lee, R.S. Rawat, Plasma Sources Sci. Technol. **14**, 368 (2005)
13. R.S. Rawat, T. Zhang, C.B.L. Phua, J.X.Y. Then, K.A. Chandra, X. Lin, A. Patran, P. Lee, Plasma Sources Sci. Technol. **13**, 569 (2004)
14. A. Serban, S. Lee, Plasma Sources Sci. Technol. **6**, 78 (1997)
15. A. Shyam, R.K. Rout, IEEE Trans. Plasma Sci. **25**, 5 (1997)
16. M. Zakaullah, I. Ahmad, N. Rashid, M.M. Beg, G. Murtaza, Plasma Phys. Control. Fusion **35**, 689 (1993)
17. M. Habibi, R. Amrollahi, M. Attaran, J. Fusion Energ. **28**, 130 (2009)
18. M. Zakaullah, G. Murtaza, I. Ahmad, F.N. Beg, M.M. Beg, M. Shabbir, Plasma Sources Sci. Technol. **4**, 117 (1995)
19. M. Zakaullah, T.J. Baig, S. Beg, G. Murtaza, Phys. Lett. A **137**, 39 (1989)